



# Activation of wnt/ $\beta$ -catenin signaling pathway down regulated osteogenic differentiation of bone marrow-derived stem cells in an anhidrotic ectodermal dysplasia patient with *EDA/EDAR/EDARADD* mutation

Dong-yu Bao <sup>a,b,1</sup>, Yun Yang <sup>a,1</sup>, Xin Tong <sup>b</sup>, Hai-yan Qin <sup>a,\*</sup>

<sup>a</sup> Department of Stomatology, the Affiliated Drum Tower Hospital of Nanjing University Medical School, 321 Zhongshan Road, Nanjing, 210008, China

<sup>b</sup> Department of Dental Implantology, Nanjing Stomatological Hospital, Medical School of Nanjing University, No.30 Zhongyang Road, Nanjing, 210008, China

## ARTICLE INFO

### Keywords:

Ectodermal dysplasia  
Osteogenesis  
Mesenchymal stem cell  
Wnt/ $\beta$ -Catenin pathway

## ABSTRACT

**Objective:** To explore the mechanism by which the Wnt/ $\beta$ -catenin pathway induces osteogenic differentiation of bone marrow-derived stem cells (BMSCs) in anhidrotic ectodermal dysplasia (AED) with an Ectodysplasin A (EDA)/EDA receptor (EDAR)/EDARADD mutation.

**Methods:** An AED patient served as the AED group, whereas the other patients without AED were included in the normal group. Peripheral venous blood collected from the AED patient was subjected to whole-genome resequencing. BMSCs from the mandible of patients with AED and normal individuals were isolated and cultured *in vitro*. Cell proliferation assay was performed to compare the growth speed of BMSCs between the AED and normal groups. CHIR-99021, an activator of the Wnt/ $\beta$ -catenin pathway and XAV-939, an inhibitor, was used to manage BMSCs in an osteogenic environment in both groups. The expression of  $\beta$ -catenin was detected by quantitative polymerase chain reaction, while that of RUNX2 was detected by western blotting. Alizarin red was used for staining.

**Results:** A novel mutation (c.152T > A in EDA) and two known mutations (c.1109T > C in EDAR and c.27G > A in EDARADD) were identified. The growth rate in the normal group was higher than that in the AED group. In the normal group, the number and size of calcified nodes and the expression of RUNX-2 increased with CHIR-99021 treatment, which could be inhibited by XAV-939. In contrast, CHIR-99021 inhibited osteogenesis in the AED group and this effect was promoted by XAV-939.

**Conclusion:** Activation of the Wnt/ $\beta$ -catenin pathway downregulates osteogenesis of BMSCs in AED patients with EDA/EDAR/EDARADD gene mutations. Further investigation in more AED patients is required, given the wide range of mutations involved in AED.

\* Corresponding author. Department of Stomatology, Affiliated Drum Tower Hospital of Nanjing University Medical School, Nanjing 210008, China.

E-mail address: [haiyanandrew@163.com](mailto:haiyanandrew@163.com) (H.-y. Qin).

<sup>1</sup> These authors contributed equally to this study.

<https://doi.org/10.1016/j.heliyon.2023.e23057>

Received 30 December 2022; Received in revised form 29 October 2023; Accepted 24 November 2023

Available online 9 December 2023

2405-8440/© 2023 Published by Elsevier Ltd.

This is an open access article under the CC BY-NC-ND license

(<http://creativecommons.org/licenses/by-nc-nd/4.0/>).

## 1. Introduction

Hypohidrotic ectodermal dysplasia (HED), also known as anhidrotic ectodermal dysplasia (AED), is an X-linked genetic disease involving the hair, teeth, nails, and sweat glands [1,2]. Cluzeau et al. [3] studied the prevalence rate of gene mutations in HED patients and concluded that 92 % of these patients experienced at least one mutation in *Ectodysplasin A (EDA)*, *EDA receptor (EDAR)*, *EDARADD*, and *WNT10A*. The appearance of HED/AED in the oral cavity is mainly manifested by tooth malformations, oligodontia/anodontia, and decreased secretory function of the glands [4]. Generally, the treatment for oligodontia or anodontia in patients with HED/AED includes removable dentures or implant-fixed/removable dentures, depending on the age of the patient [5]. Implant-fixed denture (according to the all-on-four protocol) was performed in a 20-year-old AED patient in our hospital, but two of the four implants failed 2 years after surgery because of poor osteointegration, which was different from the results of other studies which suggested that dental implants had favourable success rates in adult patients with HED/AED [4].

Osteoblast differentiation on titanium surfaces is a key step in osteointegration after implantation. Bone marrow mesenchymal stem cells (BMSCs) play an important role in osteoblast differentiation during osteointegration and are regulated by the Wnt/ $\beta$ -catenin signaling pathway. The Wnt/ $\beta$ -catenin signaling pathway also modulates osteoblast differentiation when activated by the titanium surface of dental implants [6]. Besides, it also exerts important function in regulating the proliferation and differentiation of mesodermal and ectodermal cells in the early embryo state, while EDA participates in this program [7]. Zhang et al. [8] suggested that the Wnt/ $\beta$ -catenin signaling pathway acts upstream of EDAR, the activity of which may be necessary for invoking  $\beta$ -catenin. Moreover, the EDA/NF- $\kappa$ B signaling pathway activates Wnt/ $\beta$ -catenin signaling-associated components in the mammary glands of HED patients [9]. Thus, it was suspected that implant failure in the 20-year-old patient might be related to the abnormality of the Wnt/ $\beta$ -catenin signaling pathway caused by *EDA/EDAR/EDARADD* mutation. However, there is insufficient evidence to explore the effects of BMSCs on HEDs/AEDs. Therefore, bone marrow mesenchymal stem cells (BMSCs) were isolated from the mandible of one patient to investigate the probable reasons for implant failure through the Wnt/ $\beta$ -catenin signaling pathway in this patient.

## 2. Method and materials

### 2.1. Study subjects

This study was reviewed and approved by the Ethics Committee of the Nanjing Stomatological Hospital, Medical School of Nanjing University (NO.2018NL-032). A 20-year-old male patient with tooth malformations, hypodontia, mandibular atrophy, and anhidrosis was diagnosed with AED and served as the AED group. Peripheral venous blood (4 mL) was phlebotomised from this patient and submitted to BGI Genomics Co., Ltd. (Shenzhen, China) for whole-genome resequencing. The normal group included people aged 20–30 years from the Department of Implantology in Nanjing Stomatological Hospital, excluding ectodermal dysplasia. All the experiments were performed in accordance with the Code of Ethics of the World Medical Association (*Declaration of Helsinki*). All donors agreed and provided written informed consent for the donation of materials and the medical information being submitted for publication.

### 2.2. Cells isolation

BMSCs were isolated from the cancellous mandible and bone marrow of two groups of patients who underwent implant surgery in our department with their agreement. One AED patient (aged 20 years) and three normal donors (aged 23 years, 19 years, and 21 years) who underwent dental implant surgery were included. The donors signed an informed consent form for cell isolation. The isolation of primary BMSCs was approved by the Ethics Committee of Nanjing Stomatological Hospital (NO.2018NL-032). Cancellous bone and bone marrow from the mandible were collected at the implant site after drilling the trajectory. Once the collection was completed, the tissues were rapidly seeded into  $\alpha$ -MEM (Hyclone, USA) with 1 % penicillin-streptomycin (Hyclone, USA) on ice, and subsequently delivered to the laboratory.

The isolation procedure was performed using biohazard safety equipment. The jawbone and bone marrow were placed on 60-mm dishes (Corning, USA) with 3 mL  $\alpha$ -MEM medium containing 15 % foetal bovine serum (FBS, Sciencell, USA) and 0.1 mM L-Ascorbic acid (Sigma-Aldrich, USA), and incubated at 37 °C with 5 % CO<sub>2</sub> as previously described [10]. On day 3, half of the medium was removed and new medium was added to the dishes. The entire culture medium was changed every 3 days. Adherent cells were observed on day 7. Cells were detached with 0.25 % Trypsin-EDTA (Hyclone, USA) when the cells reached 80 % of confluence, and were generated into three plates described before [10]. The cells from the three donors were pooled during the first generation to avoid individual heterogeneity, which was described by Widholz et al. [10,11].

### 2.3. Flow cytometric analysis

To identify cell types,  $5 \times 10^5$  cells at generation 3 were incubated with FITC or PE-Vio770 labelled monoclonal antibodies (Miltenyi Biotec, Germany), including FITC-CD73, FITC-CD90, PE-Vio770-CD34, and PE-Vio770-CD45, on ice for 30 min, as recommended. This assay was repeated three times. Fluorescence was analysed using a fluorescence-activated cell sorter (FACS, LSR Fortessa, BD Pharmingen, USA), and the data were analysed using FlowJo software (FlowJo V 10.0.7).

#### 2.4. Proliferation assay

Cells at generation 3 were detached and resuspended in culture medium and seeded in 96-well plates (5000 cells per well) for the CCK-8 proliferation assay. The cells were incubated for seven days, and the CCK-8 assay was performed once every 24 h. Briefly, the culture medium was replaced with 100  $\mu$ L medium containing 10  $\mu$ L CCK-8 reagent (Dojindo, Japan) according to the manufacturer's instructions and incubated at 37 °C for 1 h. The absorbance of the suspensions was measured at 450 nm using a microplate reader (SpectraMax M5, MD) to estimate the cell count. The cell count was recorded at baseline and once every 24 h thereafter. Six parallel replications were designed for technical repeats.

#### 2.5. Colony formation assay

For the colony formation assay, cells at generation 2 were detached and counted using an automated cell counter (Countess; Invitrogen).  $10^3$  cells were seeded on an average of 10 cm dish, and incubated under 5 % CO<sub>2</sub> at 37 °C for 14 days. The culture medium was changed once every three days. After 14 days, the medium was removed, and the cells were washed three times with PBS. Cells were fixed with 4 % formalin, stained with 1 % toluidine blue (Sigma-Aldrich) at room temperature overnight, and washed several times with water until the free stain was completely removed. The numbers of colonies were counted by ImageJ (V1.8.0.112 64-bit), and compared between two groups. This assay was repeated three times.

#### 2.6. CHIR-99021 and Xav-939 regulated the osteogenesis induction in vitro

Two groups of cells at generation 4 with 100 % confluency were cultured in osteogenic induction medium as control group ( $\alpha$ -MEM, 15 % FBS, 0.1 mM L-Ascorbic acid, 1.8 mM KH<sub>2</sub>PO<sub>4</sub>, 10<sup>-8</sup> M dexamethasone). In addition, to evaluate the potential effect of AED on the Wnt/ $\beta$ -catenin signaling pathway in bone formation, CHIR-99021 (3  $\mu$ M and 6  $\mu$ M, Selleck, USA) (an activator of Wnt/ $\beta$ -catenin pathway) and XAV-939 (3  $\mu$ M and 6  $\mu$ M, Selleck, USA) (an inhibitor) were added to process the cells in an osteogenic environment for 14 days in 6-well plates and 21 days in 12-well plates. The culture medium was changed once every three days. Cells in the 6-well plates cultured for 14 days were subjected to quantitative polymerase chain reaction (Q-PCR) and Western blot assays, while the 12-well plates were cultured for 21 days for Alizarin Red staining.

#### 2.7. Quantitative polymerase chain reaction (Q-PCR)

Total RNA was extracted using TRIzol Reagent kit (Invitrogen, USA) according to the manufacturer's instructions. The RNA was reverse transcribed into cDNA using the PrimeScript<sup>TM</sup> RT Reagent Kit (TAKARA, Japan) and then amplified using KAPA SYBR<sup>®</sup> FAST Q-PCR Kits (KAPA, UK) with the ABI QuantStudio<sup>TM</sup> 6 Flex system (Thermo Fisher Scientific, USA). The primer sequences were as follows: *GAPDH*: Forward: ATCACTGCCACCCAGAAG, Reverse: TCCACGACGGACACATTG; *RUNX-2*: Forward: CGCATTCCTCATCCAGTAT, Reverse: GACTGGCGGGGTGTAAGTAA;  *$\beta$ -catenin*: Forward: AAAGCGGCTGTTAGTCACTGG, Reverse: CGAGTCATTGCATCTACTGTCCAT. Q-PCR was performed in triplicate for each group, and the results were analysed using the 2<sup>- $\Delta\Delta$ ct</sup> method and normalised to *GAPDH*.

#### 2.8. Western blot assay

Western blot assay was performed as previously described [10]. Briefly, protein was extracted with RIPA lysis buffer (Beyotime Biotechnology, China) on ice, quantified using the Pierce<sup>TM</sup> BCA Protein Assay Kit (Invitrogen, USA), and mixed with 5X loading buffer (Beyotime). The mixture was heated at 95 °C for 10 min to denature the protein and then loaded into the SDS-PAGE system. The primary antibodies used were anti-RUNX-2 rabbit mAb (Cell Signaling Technology, USA) and anti-GAPDH rabbit pAb (Goodhere Biotechnology, China), while the secondary antibody was goat anti-rabbit IgG-HRP (Santa Cruz Biotechnology, USA). The fluorescence of the cell membranes was scanned using an ImageQuant Las 4000 (Life Technologies, USA). To quantify the outcome, ImageJ software was used to analyse the bands, and each band was repeated three times.

#### 2.9. Alizarin red staining

After 21 days of cell processing in 12-well plates, the culture medium was removed and the cells were fixed with 70 % isopropanol. The 12-well plate was then hydrated with pure water and stained with Alizarin Red (Sigma-Aldrich, USA). The alizarin red-positive area was calculated using ImageJ software (V1.8.0.112 64-bit) [12].

#### 2.10. Statistical analysis

GraphPad Prism 6.0 software was applied for all data analysis. The data were expressed by the mean  $\pm$  standard deviation and one-way ANOVA was used for intergroup comparison. P < 0.05 was considered statistically significant.

### 3. Results

#### 3.1. Case analysis of the AED patient

In this case, a 20-year-old male patient visited our department for restoration of anodontia (Fig. 1. A and Fig. 1B). The patient reported that he was the only AED patient in his family (Fig. 1C). During implantation, a rare amount of cancellous bone or bone marrow at the implant site was noted due to the extremely atrophic mandible (Fig. 1. D). Panoramic and cone-beam computed tomography revealed that four implants (Nobel Active, Sweden) were inserted correctly according to the all-on-4 protocol (Fig. 1. E1). Unfortunately, one implant (Fig. 1. E2, marked in red) was lost six months later. After three months, a second surgery was performed to insert an implant at the same site (Fig. 1. E3). However, an additional implant (Fig. 1. E4, marked in red) failed again 1 year after the primary surgery. A third surgery was performed, and the patient finally received an all-on-4 restoration 1 year later (Fig. 1. E5).

#### 3.2. Whole-genome resequencing

The whole-genome resequencing results revealed one missense mutation in the coding regions of *EDA*, *EDAR* and *EDARADD*, respectively. Three heterozygous mutations of *EDA*, *EDAR* and *EDARADD*, including one novel mutation (c.152T > A in *EDA*) and two known mutations (c.1109T > C in *EDAR* and c.27G > A in *EDARADD*) (Table 1.) were found [13]. The Likelihood Ratio Test (LRT), Functional Analysis Through Hidden Markov Models (FATHMM) [14], and Mutation Taster were used to predict the possibility of the disease, and the outcomes are shown in Table 1. The prediction was made by BGI Genomics Co., Ltd. (Shenzhen, China).

#### 3.3. Cells characteristics

Cells with fibroblast-like morphology were observed 7 days after seeding on a 60 mm dish. The primary cells reached 80 % confluence on day 17 and retained spindle-like morphology (Fig. 2. A).

Flow cytometric analysis showed that the expression of surface markers was similar between the two groups. The surface markers included typical BMSC (CD73 and CD90) and haematopoietic stem cell (CD34 and CD45) markers. The normal group expressed CD73 (98.9 %), CD90 (99.4 %), CD34 (1.89 %), and CD45 (1.56 %), whereas the AED group expressed CD73 (99.8 %), CD90 (99.8 %), CD34 (0.41 %), and CD45 (0.26 %) (Fig. 2. B). The results indicated that the cells in the AED patient might normally express the BMSCs specific surface markers, indicating that BMSCs existed in the jawbone marrow of the AED patient.

#### 3.4. Cells proliferation and colony formation

Cell proliferation was evaluated with CCK-8 kits using absorbance to represent the cell count. The results demonstrated a significant difference in the proliferation ability of cells between the two groups. Cells in the normal group grew faster and reached stationary phase on day 5. However, the cells of the AED patient reached the same level on day 7 (Fig. 3. A). This finding suggests that the augmentation function of BMSCs in the AED patient was lower than that in the normal group.

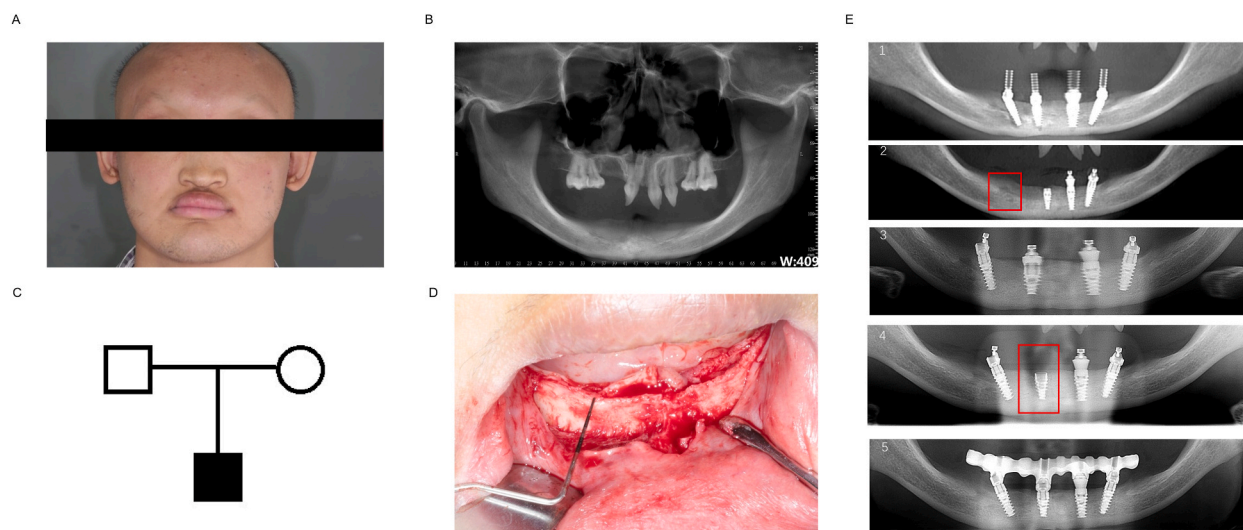


**Fig. 1.** Clinical figure of the AED patient. (A) Frontal facial image. (B) The preoperative panoramic radiograph. (C) Pedigree chart. (D) Intraoral image showed the donor site during implant surgery. (E) Panoramic of patient after surgery. E1. Immediate postoperative image. E2. Implant (Red labelled) lose after 6 months. E3. Second surgery involving an implant insertion. E4. Implant (Red labelled) failure again. E5. Restoration 1 year after the third surgery.

**Table 1**  
Summary of mutation of *EDA*, *EDAR*, *EDARADD*.

| Gene    | Nucleotide Change | Amino Acid Change | LRT | FATHMM      | Mutation Taster |
|---------|-------------------|-------------------|-----|-------------|-----------------|
| EDA     | c.152T > A        | p.Leu51Gln        | N   | D,D,D,D,D,D | D               |
| EDAR    | c.1109T > C       | p.Val370Ala       | D   | D,D,D       | P               |
| EDARADD | c.27G > A         | p.Met9Ile         | U   | T           | P               |

LRT: N-Neutral, D-Deleterious, U-Unknown. FATHMM: D-Deleterious, T-Tolerated. Mutation Taster: D-Disease causing, P-Polymorphism automatic (demonstrated in the database).

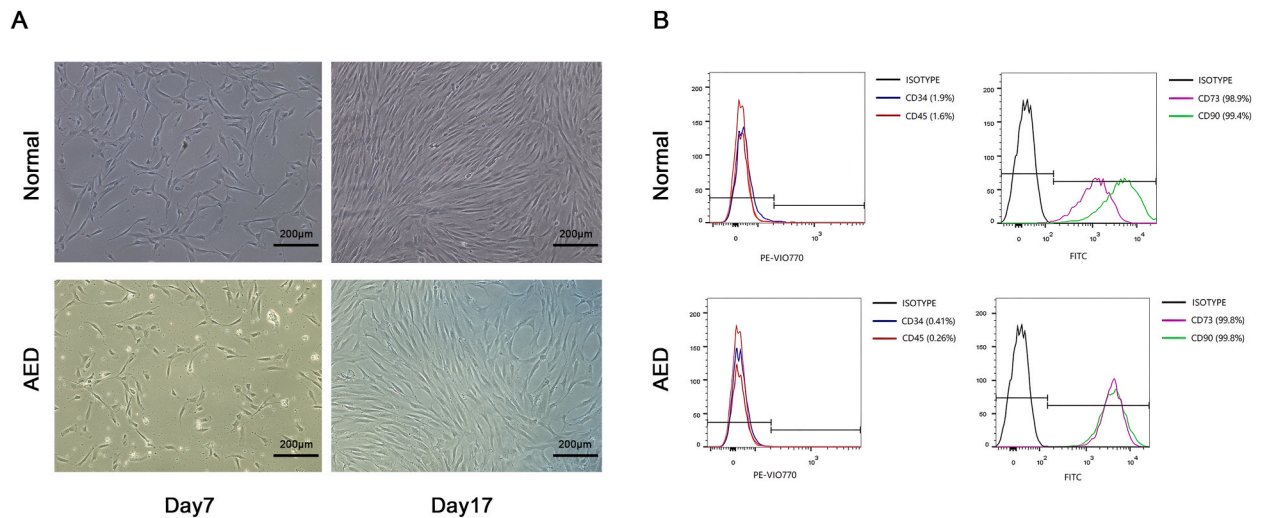


**Fig. 2.** Characteristics of the cells. (A) The fibroblast-like morphology cells could be observed at day 7 in both groups. Cells reach 80 % confluence in day 17 with fibroblast-like morphology. (B)The surface marker expression of both groups of cells showed positive expression in CD73 and CD90, and negative expression in CD34 and CD45.

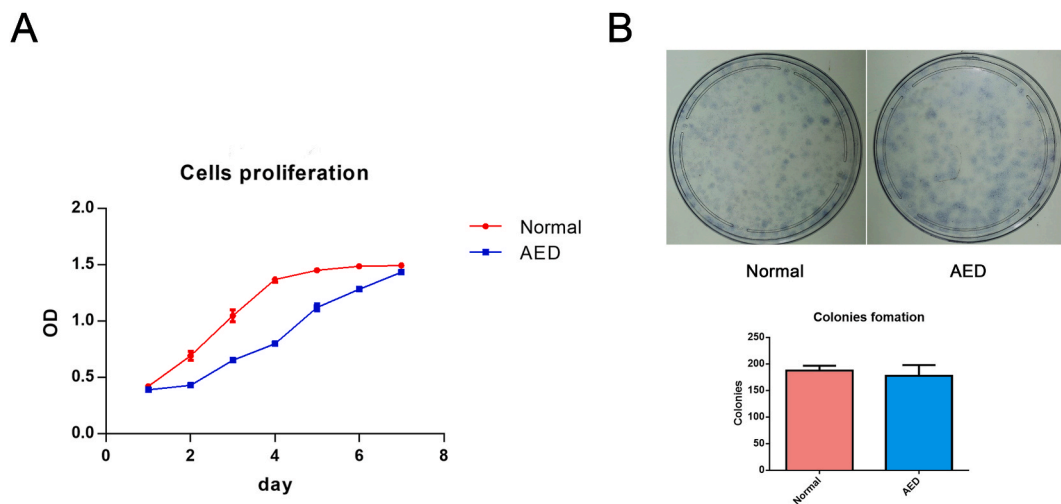


**Fig. 3.** (A) Proliferation analysis revealed that the cells in normal group grew faster and reached the stationary phase in day 5, while those in the AED group reached the same level in day 7, indicating a difference proliferation ability between the two groups. (B) Colony formation in the two groups; both could form colonies and did not differ in terms of the amounts of colonies. Data are means  $\pm$  SEM. \* means  $p < 0.05$ , \*\* means  $p < 0.01$ , \*\*\* means  $p < 0.001$ .

Colony formation analysis suggested that cell activity was not significantly different between the two groups. Cells in both groups formed colonies, and the number of colonies did not show any statistically significant difference (Fig. 3. B).

### 3.5. Q-PCR

CHIR-99021 promoted while XAV-939 suppressed the  $\beta$ -catenin expression, indicating that the Wnt/ $\beta$ -catenin signaling pathway was regulated by the activator or inhibitor in both groups (Fig. 4A).

However, the osteogenesis-related gene *RUNX-2* showed discrepant expression between the normal and AED group (Fig. 4B). The

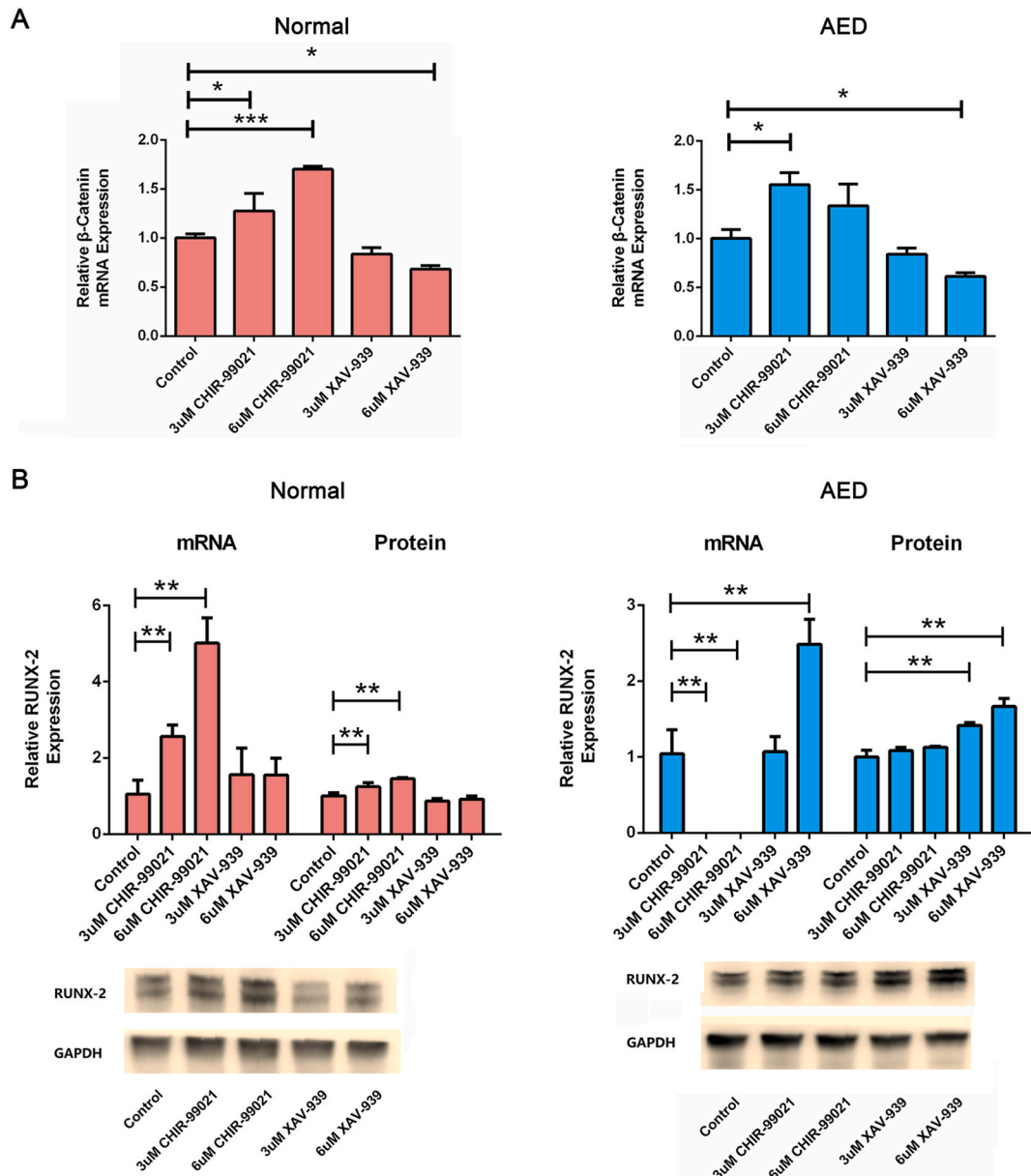


**Fig. 4.** (A) Q-PCR analysis results showed that CHIR-99021 or XAV-939 activated or inhibited  $\beta$ -catenin expression in both groups, indicating that the canonical Wnt/ $\beta$ -catenin signaling pathway is regulated by CHIR-99021 and XAV-939. (B) Q-PCR analysis and Western Blot. CHIR-99021 enhanced the *RUNX-2* gene expression in the normal group while CHIR-99021 inhibited the expression in the AED group. The *RUNX-2* expression was higher under the stimulation of XAV-939 in the AED Group. Western Blot results suggested that CHIR-99021 upregulated the *RUNX-2* protein expression in the normal group. XAV-939 increased the *RUNX-2* protein expression in the AED group. Non-adjusted images of Western Blot were provided in Supplementary material (See in Supplement1 and Supplement2). Data are means  $\pm$  SEM. \* means  $p < 0.05$ , \*\* means  $p < 0.01$ , \*\*\* means  $p < 0.001$ .

mRNA expression of *RUNX-2* was markedly increased in the normal group after incubation with CHIR-99021, especially at a concentration of 6  $\mu$ M. In contrast, CHIR-99021 obviously inhibited the expression of *RUNX-2* in the AED group. Furthermore, XAV-939 incubated BMSCs from the normal group showed no statistically significant difference relative to the osteogenic medium only, but 6 $\mu$ M XAV-939 strongly increased the expression of *RUNX-2*. These findings revealed that there was a significant difference in the effect of CHIR-99021 and XAV-939 between the normal and AED groups.

### 3.6. Western blot assay

The Western blot bands for the two groups were assessed (Fig. 4B). Non-adjusted images of Western Blot were provided in Supplementary material (See in Supplement1 and Supplement2). In the normal group, CHIR-99021 enhanced the expression of *RUNX-2*, especially at a concentration of 6 $\mu$ M, which showed the same trend as the results of Q-PCR. However, CHIR-99021 did not reduce the expression of *RUNX-2* protein in the AED group, as in the Q-PCR analysis, while XAV-939 enhanced the expression of *RUNX-2* in the AED group.

### 3.7. Alizarin red staining

Alizarin red staining represents the mineralisation ability of the cells *in vitro*. These results indicated that both groups formed mineralisation nodes *in vitro* in an osteogenic environment. However, CHIR-99021 promoted osteogenesis and inhibited node formation in the normal and AED groups, respectively. XAV-939 slightly reduced the osteogenesis effect in the normal group while extraordinarily increasing that in the AED group (Fig. 5. A). The percentage of positive areas was calculated using ImageJ software (Fig. 5. B). The opposite effects of CHIR-99021 and XAV-939 on bone formation showed similar trends in *RUNX-2* expression. The

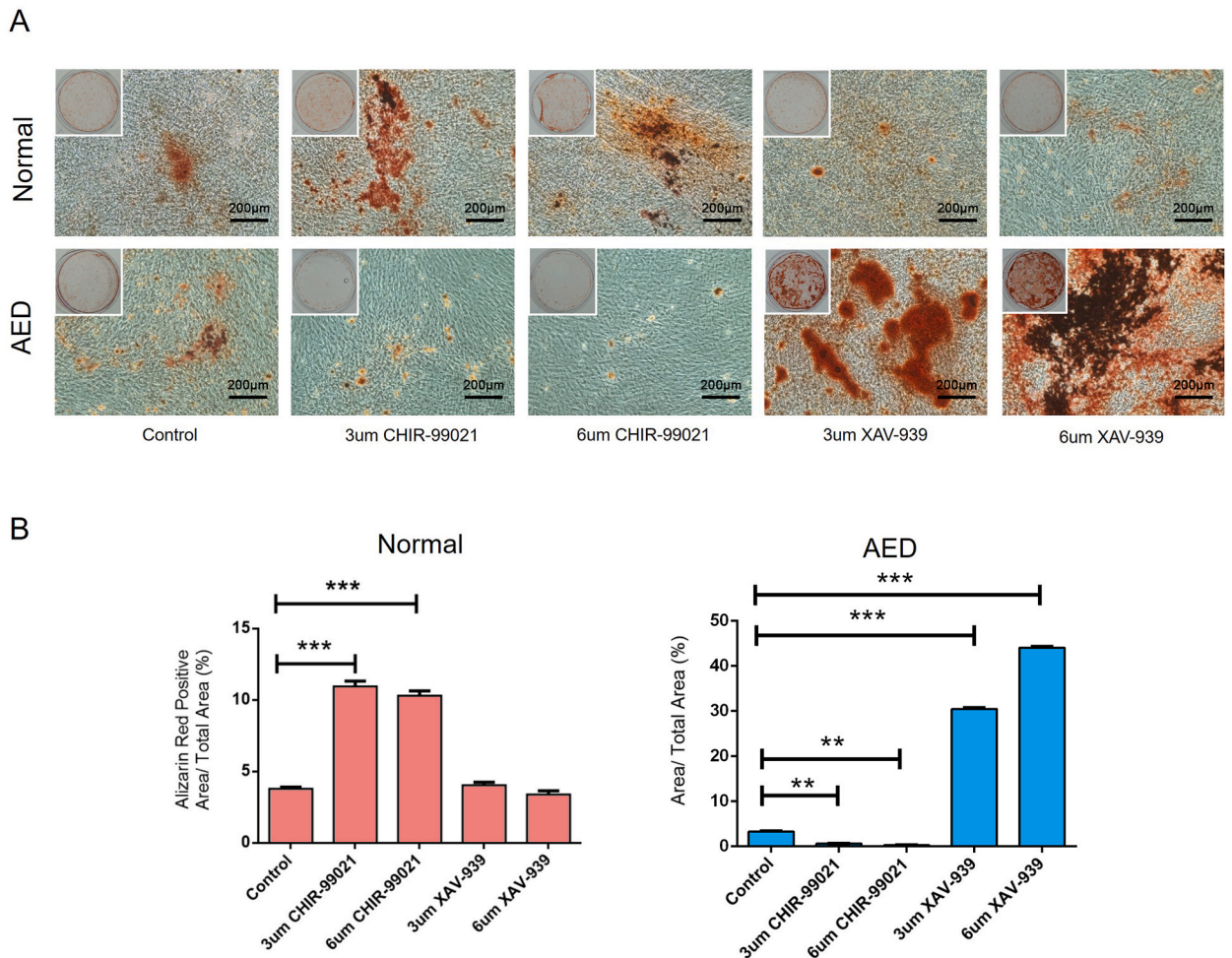


**Fig. 5.** (A) Alizarin red staining revealed that CHIR-99021 increased the osteogenesis ability in the normal group and decreased it in the AED group. Conversely, XAV-939 decreased the osteogenesis ability in the normal group and decreased the ability in the AED group. (B) Statistic results of the area of the nodes. Data are means  $\pm$  SEM. \* means  $p < 0.05$ , \*\* means  $p < 0.01$ , \*\*\* means  $p < 0.001$ .

above findings indicate that the Wnt signaling pathway may play different roles in the osteogenesis of BMSC between the normal and AED groups.

#### 4. Discussion

Ectodermal dysplasia (ED) is defined as a series of related syndromes caused by 77 different identified genetic mutations and can be inherited in the next generation [15]. More than 170 types of ED have been described, of which X-linked HED or AED is the most common, depending on the secretion of perspiration [16]. The incidence of HED or AED is 1:17,000 in live births [17], but N. Ngoc et al. reported that the prevalence of HED is only 1:1,000,000 in the general population [18]. 92 % of these patients have at least one gene mutation in *EDA*, *EDAR*, *EDARADD* and *WNT10A* [3]. Whole-genome resequencing was initially performed for this AED patient, and one novel mutation (c.152T > A in *EDA*) and two known mutations (c.1109T > C in *EDAR* and c.27G > A in *EDARADD*) were found in the coding sequence (CDS). No mutations in CDS of *WNT10A* has been observed. The c.152T > A mutation leads to the Leu<sup>51</sup> of transmembrane protein EDA (isoform 1) to Gln according to the database (<https://www.ncbi.nlm.nih.gov/gene/1896>). Prediction software revealed that the c.152T > A mutation may lead to disease. Liu [19] reported a novel missense mutation, p. S305R, in *EDA* which led to an insoluble EDA1 protein. The pathogenesis of this c.152T > A mutation requires further research.

The EDA-1 protein is a significant component encoded by the gene *EDA* located on the X chromosome. It binds to *EDAR* as a ligand and raises the cascade of the NF- $\kappa$ B signaling pathway to regulate cell apoptosis [20]. Wnt/ $\beta$ -catenin signaling plays a critical role in the proliferation and differentiation of mesenchymal stem cells (MSCs), thus inducing osteogenesis and tooth development [21,22]. It can also activate Wnt/ $\beta$ -catenin signaling-associated components in the mammary glands of HED patients [9], but the mechanism through Wnt/ $\beta$ -catenin signaling in ectopic teeth remains unclear. Wnt/ $\beta$ -catenin signaling is an important pathway in osteoblastogenesis and osseointegration of titanium dental implants. Primary stability of the implant is essential for osseointegration. Implants inserted without primary stability upregulate the expression of sclerostin, an inhibitor of the Wnt/ $\beta$ -catenin signaling pathway, and then cause failure of osseointegration of implants [23]. Titanium also regulates the Wnt/ $\beta$ -catenin signaling pathway to induce osteoblast differentiation which is highly associated with BMSCs [24]. The crucial role of the Wnt/ $\beta$ -catenin signaling pathway in tooth genesis, osteogenesis, and osteoblast differentiation of BMSCs in osseointegration between titanium dental implants and alveolar bones has been previously confirmed. In this study, it was assumed that mutations in *EDA*, *EDAR*, *EDARADD* probably affected these processes. BMSCs were originally isolated from a 20-year-old AED patient and the osteogenesis abilities through the Wnt/ $\beta$ -catenin signaling pathway were explored to determine the association between *EDA* mutation, Wnt/ $\beta$ -catenin signaling pathway, and the function of BMSCs in AED/HED patients.

The types of cells isolated were identified. In the flow cytometry analysis, the expression of the surface markers CD73 and CD90 in BMSCs in the AED group showed no significant difference relative to those in the normal group. CD90 is distributed in any type of mesenchymal stem cell and is able to activate proliferation to cure wounds [25]. Moraes et al. (Moraes et al., 2016) suggested that CD90 can prevent stem cell differentiation as an inhibitor. The high expression level of CD90 represents the stemness of the cells and decreases when the cells initiate differentiation [26]. Therefore, the cytometry data showed that there was no significant difference in the stemness between the two groups. Additionally, the proliferation of AED BMSCs was lower in the AED group than that in the normal group. The Wnt signaling pathway can regulate the stem cell proliferation [27]. In AED cells, proliferation may be inhibited by the Wnt pathway, resulting in a lack of stem cells to form new bone, which still needs to be further verified.

The Wnt signaling activator CHIR-99021 and inhibitor XAV-939 were used to regulate the pathway [28,29], and PCR data specific to  $\beta$ -catenin expression confirmed the effectiveness of both.  $\beta$ -catenin is required in the canonical Wnt signaling pathway in the cytoplasm, where  $\beta$ -catenin is translocated into the nucleus and then activates the downstream gene of Wnt [30] after binding to LEF/TCF as a transcription factor. The effects of these activators and inhibitors on osteogenesis of BMSCs were analysed in the normal and AED groups. Consistent with previous studies, the Wnt/ $\beta$ -catenin signaling pathway plays a regulatory role in bone formation enhancement in different cell types [31,32]. The canonical Wnt signaling pathway promotes *RUNX2* gene expression via the  $\beta$ -catenin/TCF complex and stimulates bone formation in mice [33]. *RUNX2* is a key downstream regulator that is activated by the canonical Wnt/ $\beta$ -catenin pathway. In this study, the osteogenesis results in the normal group demonstrated the same trend as those in other studies. However, the effect of the canonical Wnt/ $\beta$ -catenin signaling pathway on osteogenesis has been argued by Harada et al. who suggested that several markers of osteogenic differentiation were downregulated by Wnt [34]. Moreover, osteogenic differentiation was strongly inhibited by Wnt3a and transduction of Wnt1 in hMSC, as reported by Liu et al. [35]. Hence, the most crucial marker *RUNX2* in gene and protein expression was examined in the present study, and the results revealed that *RUNX2* expression was promoted under the effect of CHIR-99021, whereas it was inhibited by XAV-939 in the normal group. However, the *RUNX2* expression in AED group was inhibited when Wnt/ $\beta$ -catenin signaling pathway was activated by CHIR-99021. As mentioned before, Titanium could upregulate the Wnt/ $\beta$ -catenin signaling pathway to induce osteoblast differentiation resulting in osseointegration, which was a crucial step in implant restoration [24]. *RUNX2* was essential for osteoblast differentiation and bone formation, Hata et al. demonstrated that Titanium-MAPK-*RUNX2* pathway might play important roles in osseointegration [36]. Thus, the Wnt/ $\beta$ -catenin signaling activated by Titanium might downregulate the transcription of *RUNX2* and hence reduced the osseointegration of dental implant, finally causing implant failure. Furthermore, *RUNX2* could regulate the proliferation of osteoblast progenitors and their differentiation into osteoblasts via Wnt/ $\beta$ -catenin signaling pathway [37]. The reduce expression of *RUNX2* could inhibit the differentiation of BMSCs to osteoblastic cells, resulting a negative effect on osteogenesis.

Osteogenesis of AED BMSCs was suppressed when Wnt/ $\beta$ -catenin was activated, which indicated that the Wnt/ $\beta$ -catenin pathway might play a different role in BMSCs from normal people or AED patients. Xu et al. suggested that downstream  $\beta$ -catenin pathway activation was reduced in the absence of *WNT10A*, which occurred in patients with *WNT10A* mutations [38]. However, the

whole-gene sequencing results of this patient showed no *WNT10A* gene mutations. This suggests that the opposite result may be associated with *EDA/EDAR/EDARADD* gene mutation. However, the underlying mechanism among Wnt/ $\beta$ -catenin, *EDA/EDAR/EDARADD* gene mutation and bone development was still unclear. In our study, the expression of  $\beta$ -catenin indicated that the Wnt/ $\beta$ -catenin pathway was activated by CHIR-99021 and inhibited by XAV-939 both in Normal group and AED group, but the expression of RUNX2 and the osteogenesis outcome were different between Normal group and AED group. This result might be associated with *EDA/EDAR/EDARADD* gene mutation. The Wnt/ $\beta$ -catenin pathway is required for *EDA/EDAR/NF- $\kappa$ B* signaling and *EDA* is a direct target of  $\beta$ -catenin [8], and Zhang et al. demonstrated that *EDAR* could deactivate the Wnt/ $\beta$ -catenin pathway, and the silencing *EDAR* showed upregulation of  $\beta$ -catenin [39]. Hence, we supposed that the mutation of *EDAR* might disordered the expression of  $\beta$ -catenin and resulted negative feedback to bone formation. However, this hypothesis needs more experiments to be strictly proved. Besides, the canonical Wnt/ $\beta$ -catenin signaling pathway showed multifaceted effects in bone development depending on different environment. Suppressing Wnt/ $\beta$ -catenin signaling pathway could also promote the osteogenic differentiation of rat bone marrow-derived mesenchymal stem cells [40], and Almasoud et al. found that XAV-939 could enhance osteoblastogenesis and mineralisation in hMSC-TERT (Telomerase Reverse Transcriptase gene) [41]. These multifaceted effects might also be the reason why our study showed discrepancy results in Normal group and AED group. Most studies have revealed that Wnt/ $\beta$ -catenin is crucial for ectodermal development and formation by regulating *EDA* family, especially in the tooth and hair follicle formation [42–45]. However, the regulation of osteo-related morphogenesis in the *EDA* family has not yet been explored. Although the *EDA* family seems unrelated to osteogenesis, a genome study showed that mouse mandible length was associated with *EDAR* genotype [46]. The mandible is a special bone originally derived from the neural crest, a dorsal region of the neural fold [47]. Neural crest cells have been confirmed as a group of multipotent cells *in vivo* that undergo epithelial-to-mesenchymal transformation [48]. Studies have indicated that the mandible originates both ectodermally and mesodermally, which is quite different from other bones (only mesodermally). This may explain why the HED/AED patients in this study appeared normal in other skeletons but suffered from extreme mandibular atrophy.

## 5. Conclusion

In this study, a novel mutation in the coding sequence of *EDA* was identified in a 20-year-old AED patient. The proliferation of BMSCs from this AED patient was significantly decreased relative to that of normal BMSCs. The activation of the Wnt/ $\beta$ -catenin signaling pathway may downregulate osteogenesis in AED patients with *EDA/EDAR/EDARADD* gene mutations. However, owing to the rarity of HED/AED, only one case of HED has been assessed in our unit to date. BMSCs obtained from a single AED patient are not representative of all AED patients, given the wide range of mutations involved in these diseases. Despite these insufficiencies, we determined some valuable information about the mechanism of Wnt/ $\beta$ -catenin signaling in AED patients, which may elucidate a new direction to further explore the mechanism of Wnt/ $\beta$ -catenin signaling in HED/AED and treat these patients.

## Ethics approval and consent to participate

This study was reviewed and approved by the Ethics Committee of the Nanjing Stomatological Hospital, Medical School of Nanjing University (NO.2018NL-032). All donors agreed and provided written informed consent for the donation of materials and the medical information being submitted for publication.

## Data availability statement

The Data of this study will be made available on request.

## CRediT authorship contribution statement

**Dong-yu Bao:** Writing - original draft, Methodology, Investigation, Formal analysis, Conceptualization. **Yun Yang:** Writing - review & editing, Software, Formal analysis. **Xin Tong:** Resources. **Hai-yan Qin:** Writing - review & editing, Project administration, Funding acquisition, Data curation, Conceptualization.

## Declaration of competing interest

The authors declare that they have no known competing financial interests or personal relationships that could have appeared to influence the work reported in this paper.

## Acknowledgement

This study was supported by the National Natural Science Foundation of China (Grant No. 81200770).

## Appendix A. Supplementary data

Supplementary data to this article can be found online at <https://doi.org/10.1016/j.heliyon.2023.e23057>.

## References

- [1] N. Freire-Maia, Ectodermal dysplasias revisited, *Acta Genet. Med. Gemellol.* 26 (2) (1977) 121–131.
- [2] N. Freire-Maia, Ectodermal dysplasias, *Hum. Hered.* 21 (4) (1971) 309–312.
- [3] C. Cluzeau, et al., Only four genes (EDA1, EDAR, EDARADD, and WNT10A) account for 90% of hypohidrotic/anhidrotic ectodermal dysplasia cases, *Hum. Mutat.* 32 (1) (2011) 70–72.
- [4] Y. Wang, et al., Clinical outcomes of implant therapy in ectodermal dysplasia patients: a systematic review, *Int. J. Oral Maxillofac. Surg.* 45 (8) (2016) 1035–1043.
- [5] A.J. Hickey, T.J. Vergo Jr., Prosthetic treatments for patients with ectodermal dysplasia, *J. Prosthet. Dent* 86 (4) (2001) 364–368.
- [6] S. Lumetti, et al., Pharmacological GSK-3beta inhibition improves osteoblast differentiation on titanium surfaces, *J. Biol. Regul. Homeost. Agents* 28 (3) (2014) 489–495.
- [7] O. Haara, et al., Ectodysplasin and Wnt pathways are required for salivary gland branching morphogenesis, *Development* 138 (13) (2011) 2681–2691.
- [8] Y. Zhang, et al., Reciprocal requirements for EDA/EDAR/NF-kappaB and Wnt/beta-catenin signaling pathways in hair follicle induction, *Dev. Cell* 17 (1) (2009) 49–61.
- [9] M. Voutilainen, et al., Ectodysplasin/NF-kB promotes mammary cell fate via wnt/ $\beta$ -catenin pathway, *PLoS Genet.* 11 (11) (2015), e1005676.
- [10] A. Shi, et al., Small molecule inhibitor of TGF- $\beta$  signaling enables robust osteogenesis of autologous GMSCs to successfully repair minipig severe maxillofacial bone defects, *Stem Cell Res. Ther.* 10 (1) (2019) 172.
- [11] B. Widholz, et al., Pooling of patient-derived mesenchymal stromal cells reduces inter-individual confounder-associated variation without negative impact on cell viability, proliferation and osteogenic differentiation, *Cells* 8 (6) (2019).
- [12] S. Patnirapong, et al., Assessment of bisphosphonate treated-osteoblast behaviors by conventional assays and a simple digital image analysis, *Acta Histochem.* 123 (1) (2021), 151659.
- [13] L. Zhang, et al., Comparative analysis of rare EDAR mutations and tooth agenesis pattern in EDAR- and EDA-associated nonsyndromic oligodontia, *Hum. Mutat.* 41 (11) (2020) 1957–1966.
- [14] H.A. Shihab, et al., Predicting the functional, molecular, and phenotypic consequences of amino acid substitutions using hidden Markov models, *Hum. Mutat.* 34 (1) (2013) 57–65.
- [15] N.A. Pagnan, A.F. Visinoni, Update on ectodermal dysplasias clinical classification, *Am. J. Med. Genet.* 164A (10) (2014) 2415–2423.
- [16] M. Priolo, C. Lagana, Ectodermal dysplasias: a new clinical-genetic classification, *J. Med. Genet.* 38 (9) (2001) 579–585.
- [17] J. Reyes-Realí, et al., Hypohidrotic ectodermal dysplasia: clinical and molecular review, *Int. J. Dermatol.* 57 (8) (2018) 965–972.
- [18] V.T.N. Ngoc, et al., Clinical, radiographic, and genetic characteristics of hypohidrotic ectodermal dysplasia: a cross-sectional study, *Clin. Genet.* 94 (5) (2018) 484–486.
- [19] G. Liu, et al., A novel missense mutation p.S305R of EDA gene causes XLHED in a Chinese family, *Arch. Oral Biol.* 107 (2019), 104507.
- [20] C.Y. Cui, D. Schlessinger, EDA signaling and skin appendage development, *Cell Cycle* 5 (21) (2006) 2477–2483.
- [21] K. Wang, et al., BRD4 induces osteogenic differentiation of BMSCs via the Wnt/ $\beta$ -catenin signaling pathway, *Tissue Cell* 72 (2021), 101555.
- [22] P. Duan, L.F. Bonewald, The role of the wnt/ $\beta$ -catenin signaling pathway in formation and maintenance of bone and teeth, *Int. J. Biochem. Cell Biol.* 77 (Pt A) (2016) 23–29.
- [23] F.L. da Silva, et al., Preliminary findings on the role of sclerostin in the osseointegration process around titanium implants, *Int. J. Oral Maxillofac. Implants* 31 (6) (2016) 1298–1302.
- [24] R.P.F. Abuna, et al., The Wnt/ $\beta$ -catenin signaling pathway is regulated by titanium with nanotopography to induce osteoblast differentiation, *Colloids Surf. B Biointerfaces* 184 (2019), 110513.
- [25] A. Saalbach, et al., Novel fibroblast-specific monoclonal antibodies: properties and specificities, *J. Invest. Dermatol.* 106 (6) (1996) 1314–1319.
- [26] T.T. Sibov, et al., Mesenchymal stem cells from umbilical cord blood: parameters for isolation, characterization and adipogenic differentiation, *Cytotechnology* 64 (5) (2012) 511–521.
- [27] J.K. Van Camp, et al., Wnt signaling and the control of human stem cell fate, *Stem Cell Rev.* 10 (2) (2014) 207–229.
- [28] X. Lian, et al., Insulin inhibits cardiac mesoderm, not mesendoderm, formation during cardiac differentiation of human pluripotent stem cells and modulation of canonical Wnt signaling can rescue this inhibition, *Stem Cell.* 31 (3) (2013) 447–457.
- [29] W.H. Lien, et al., In vivo transcriptional governance of hair follicle stem cells by canonical Wnt regulators, *Nat. Cell Biol.* 16 (2) (2014) 179–190.
- [30] B.T. MacDonald, K. Tamai, X. He, Wnt/beta-catenin signaling: components, mechanisms, and diseases, *Dev. Cell* 17 (1) (2009) 9–26.
- [31] F. Morvan, et al., Deletion of a single allele of the Dkk1 gene leads to an increase in bone formation and bone mass, *J. Bone Miner. Res.* 21 (6) (2006) 934–945.
- [32] P. ten Dijke, et al., Osteocyte-derived sclerostin inhibits bone formation: its role in bone morphogenetic protein and Wnt signaling, *J. Bone Joint Surg Am* 90 (Suppl 1) (2008) 31–35.
- [33] T. Gaur, et al., Canonical WNT signaling promotes osteogenesis by directly stimulating Runx2 gene expression, *J. Biol. Chem.* 280 (39) (2005) 33132–33140.
- [34] S. Harada, G.A. Rodan, Control of osteoblast function and regulation of bone mass, *Nature* 423 (6937) (2003) 349–355.
- [35] G. Liu, et al., Canonical Wnts function as potent regulators of osteogenesis by human mesenchymal stem cells, *J. Cell Biol.* 185 (1) (2009) 67–75.
- [36] K. Hata, et al., Osteoblast response to titanium regulates transcriptional activity of Runx2 through MAPK pathway, *J. Biomed. Mater. Res.* 81 (2) (2007) 446–452.
- [37] T. Komori, Regulation of proliferation, differentiation and functions of osteoblasts by Runx2, *Int. J. Mol. Sci.* 20 (7) (2019).
- [38] M. Xu, et al., WNT10A mutation causes ectodermal dysplasia by impairing progenitor cell proliferation and KLF4-mediated differentiation, *Nat. Commun.* 8 (2017), 15397.
- [39] X. Zhang, et al., Tumor suppressor gene XEDAR promotes differentiation and suppresses proliferation and migration of gastric cancer cells through upregulating the RELA/LXR $\alpha$  Axis and deactivating the wnt/ $\beta$ -catenin pathway, *Cell Transplant.* 30 (2021), 963689721996346.
- [40] Z. Sun, et al., Semaphorin 3A promotes the osteogenic differentiation of rat bone marrow-derived mesenchymal stem cells in inflammatory environments by suppressing the Wnt/ $\beta$ -catenin signaling pathway, *J. Mol. Histol.* 52 (6) (2021) 1245–1255.
- [41] N. Almasoud, et al., Author Correction: tankyrase inhibitor XAV-939 enhances osteoblastogenesis and mineralization of human skeletal (mesenchymal) stem cells, *Sci. Rep.* 11 (1) (2021) 4559.
- [42] J. Huelsken, et al., beta-Catenin controls hair follicle morphogenesis and stem cell differentiation in the skin, *Cell* 105 (4) (2001) 533–545.
- [43] S.E. Millar, Molecular mechanisms regulating hair follicle development, *J. Invest. Dermatol.* 118 (2) (2002) 216–225.
- [44] T. Andl, et al., WNT signals are required for the initiation of hair follicle development, *Dev. Cell* 2 (5) (2002) 643–653.
- [45] F. Liu, et al., Wnt/beta-catenin signaling directs multiple stages of tooth morphogenesis, *Dev. Biol.* 313 (1) (2008) 210–224.
- [46] K. Adhikari, et al., A genome-wide association scan implicates DCHS2, RUNX2, GLI3, PAX1 and EDAR in human facial variation, *Nat. Commun.* 7 (2016), 11616.
- [47] P.A. Trainor, R. Krumlauf, Patterning the cranial neural crest: hindbrain segmentation and Hox gene plasticity, *Nat. Rev. Neurosci.* 1 (2) (2000) 116–124.
- [48] A. Baggiolini, et al., Premigratory and migratory neural crest cells are multipotent in vivo, *Cell Stem Cell* 16 (3) (2015) 314–322.